THE MULTI-FREQUENCY DIAGONALIZED CONTRAST SOURCE METHOD FOR ELECTROMAGNETIC INVERSION

A. Casagranda[1], D. Franceschini[1], A. Massa[1], P.M. van den Berg[2], A. Abubakar[3], and T.M. Habashy[3]

[1]*Dep. of Information and Communication Technologies, University of Trento, Via Sommarive 14, Povo 38050, Italy*
[2]*Faculty of Applied Science, Delft University of Technology, Lorentzweg 1, Delft 2628 CJ, The Netherlands*
[3]*Schlumberger-Doll Research, 36 Old Quarry Road, Ridgefield, CT, 06877, U.S.A.*

ABSTRACT

Inverse scattering problems deal with the determination of the constitutive parameters of the unknown objects embedded in a known background medium. In this problem, the configuration is illuminated by a single frequency wave-field and the scattered field is measured in an external observation domain. The inversion of this data is well-known to be non-linear and ill-posed. Furthermore, the retrievable information is limited. In order to overcome such drawbacks, multi-frequency data can be used by exploiting the Maxwellian dispersion relationships. However, the use of the set of multi-frequency data significantly increases the computational burden of the inversion process. Recently, the so-called Diagonalized Contrast Source Inversion (DCSI) method is introduced to efficiently solve the inverse problem. In this method, instead of solving the full non-linear problem, a three-linear-step procedure is carried out to significantly reduce the overall computational time. In order to further enhance the DCSI method, in this paper it has been extended for dealing with multi-frequency data.

Key words: non-linear inversion; multi-frequency imaging; iterative technique.

1. INTRODUCTION

The problem of determining the electromagnetic proprieties of an unknown region by means of illuminating electromagnetic waves has been a field of intensive studies. The ways to solve this problem can be divided into two main categories. The first category concerns with techniques based on linearization ([1]) of the problem. The other category regards nonlinear techniques that recast the problem as the minimization of a cost functional (see, e.g., [2]).

In a recent work, Abubakar *et al.* [3] proposed two computational effective strategies for the solution of the full non-linear problem. The methods are called the Diagonalized Contrast Source Inversion (DCSI). These methods are based on: (a) the source-type integral equation formulation [4], (b) a robust iterative method for Born inversion [5] and (c) the diagonal approximation of the scattering operator [6]. The aim of the DCSI methods is to reduce the overall computational time by transforming the nonlinear inverse problem into a sequence of linear inversion problems that are far more simple to be solved. The numerical results both for electromagnetic and elastic wave inversion reported in [3, 7] highlight the effectiveness of these approaches as well as the favorable trade-off between complexity and reconstruction accuracy. The results obtained are comparable with those obtainable using a fully nonlinear procedure but requiring only the same or twice the computational burden of the linear techniques.

In this paper, the method is extended to incorporate the multi-frequency data. In the scientific literature on inverse problems, two main strategies have been proposed to successfully exploit the availability of multi-frequency data. The first is called the frequency-hopping approach [8]. This technique uses the data from one frequency as the initial guesses for the next (usually at an higher frequency) frequency inversion process. The alternative technique consists of processing all the available data at the same time as done, for instance, in [9]. In such a case, the definition of the cost functional is modified by introducing the summation over the different frequency data set. In this paper we employ the simultaneous frequency inversion approach since it is more robust than the frequency-hopping approach. After presenting the theory of the DCSI multi-frequency inversion approach, selected numerical results will be presented in order to analyze the performances of the proposed technique.

2. SINGLE-FREQUENCY DCSI METHOD

We consider the two-dimensional inverse scattering problem where the scattering objects of arbitrary cylindrical cross-section are contained in a homogeneous, possibly lossy, bounded domain D. We assume that the scattering objects are radiated successively by a number of incident fields $u_{k,j}^{inc}$ originating from sources with different oper-

Proc. 'EuCAP 2006', Nice, France
6–10 November 2006 (ESA SP-626, October 2006)

ating radial frequencies ω_k, $k = 1, 2, \ldots$, and different source positions $j = 1, 2, \ldots$.

We first consider the single-frequency inversion problem. Then, for each frequency the inverse problem is formulated through the domain integral equations (see, e.g., Colton and Kress [10]) that, using symbolic notation, are written as the *object equation*

$$u^{inc}_{k,j} = u_{k,j} - G^D_k \chi_k u_{k,j}, \tag{1}$$

and the *data equation*

$$f_{k,j} = G^S_k \chi_k u_{k,j}\,, \tag{2}$$

where

$$G^{D,S}_k w_{k,j} = \mathrm{Re}(k^2_{b_k}) \int_D g_k(\mathbf{p}, \mathbf{q}) w_{k,j}(\mathbf{q}) dv(\mathbf{q}).$$

The superscripts D and S refer to the field point position $\mathbf{p}$ in the domains D and S, respectively. On these domains the norms and inner products are defined in the L^2-norm sense. Further g_k is the known Green function with wavenumber

$$k_{b_k} = \omega_k \sqrt{(\epsilon_b + \mathrm{i}\frac{\sigma_b}{\omega_k})\mu_b}, \tag{3}$$

where ϵ_b, σ_b and μ_b denote the permittivity, conductivity and permeability of the background medium. The frequency dependent contrast is denoted by

$$\chi_k = \frac{\epsilon(\mathbf{p}) - \epsilon_b}{\epsilon_b} + \mathrm{i}\frac{\sigma(\mathbf{p}) - \sigma_b}{\omega_k \epsilon_b}. \tag{4}$$

Formally, the solution of the problem is obtained by solving Eq. (2) with $u_{k,j}$ obtained from Eq. (1),

$$u_{k,j} = L^{-1}_k u^{inc}_{k,j}, \quad \text{where} \quad L_k = I - G^D_k \chi_k\,. \tag{5}$$

The solution of the problem is greatly simplified if the operator $\chi_k L^{-1}_k u^{inc}_{k,j}$ is approximated by a diagonal operator η_k,

$$w_{k,j} = \chi_k L^{-1}_k u^{inc}_{k,j} \approx \eta_k u^{inc}_{k,j}. \tag{6}$$

The aim of the DCSI methods is to solve the nonlinear inverse problem by solving a sequence of linear inverse problems that are far more simple and fast to compute. This can be achieved using the source-type integral equation approach by inverting for the contrast sources $w_{k,j}$ from the data equation subject to the constraint that the full contrast operator is dominated by a diagonal form given by Eq. (6). This can be affected by introducing a method based on the contrast source inversion, as implemented in Section IV of [5]. Such a method does not require *a priori* knowledge and provides a stable inversion result through the introduction of the following two-term cost functional

$$F^I_{k;n} = \frac{\sum_j \|f_{k,j} - G^S_k w_{k,j;n}\|^2_S}{\sum_j \|f_{k,j}\|^2_S} + \frac{\sum_j \|\eta_{k;n} u^{inc}_{k,j} - w_{k,j;n}\|^2_D}{\sum_j \|\eta_{k;n-1} u^{inc}_{k,j}\|^2_D}, \tag{7}$$

where in each iteration, $n = 1, 2, \ldots, N$, the contrast source $w_{k,j;n}$ and the diagonal operator $\eta_{k;n}$ have to be estimated. It has been shown in [5] that a robust solution is obtained by an alternating direction minimization scheme in which $w_{k,j}$ and η_k are alternately updated resulting in a continues reduction of the above cost function after each update. The contrast sources are updated by a conjugate gradient algorithm, in which an explicit update for η_k is obtained after each step. This explicit update is given by

$$\eta_{k;n} = \frac{\sum_j w_{k,j;n} \overline{u}^{inc}_{k,j}}{\sum_j |u^{inc}_{k,j}|^2}, \tag{8}$$

After solving for $w_{k,j} = w_{k,j,N}$, the total wave-fields $u_{k,j}$ in D are simply computed from Eq. (1):

$$u^{inv}_{k,j} = u^{inc}_{k,j} + G^D_k \chi_k w_{k,j;N}, \tag{9}$$

and the contrast function is reconstructed from

$$\chi_k = \frac{\sum_j w^{inv}_{k,j;n} \overline{u}^{inv}_{k,j}}{\sum_j |u^{inv}_{k,j}|^2}. \tag{10}$$

Note that, the diagonal operator η_k in the object equation plays the role of regularization of the whole cost functional providing remarkable improvement (see [3]) with respect to the standard Born inversion procedure [5]. The only additional step is the computation of the final quantities $u^{inv}_{k,j}$ and χ_k whose cost is negligible compared to the total computational burden. The present method is denoted as the DCSI method I.

The DCSI method II consists of two parts. The first step is identical to the DCSI method I up to the computation of field $u^{inv}_{k,j}$. Instead of computing the contrast function using Eq. (10), the following cost functional is defined and iteratively minimized using the total internal field $u^{inv}_{k,j}$, computed at the end of DCSI-I,

$$F^{II}_{k;n} = \frac{\sum_j \|f_{k,j} - G^S_k w_{k,j;n}\|^2_S}{\sum_j \|f_{k,j}\|^2_S} + \frac{\sum_j \|\chi_{k;n} u^{inv}_{k,j} - w_{k,j;n}\|^2_D}{\sum_j \|\chi_{k;n-1} u^{inv}_{k,j}\|^2_D}. \tag{11}$$

Further, we apply the multiplicative regularization technique with a weighted L_2-norm regularization [11]. Then, the cost functional is given by

$$\mathcal{C}_{k;n} = F^{II}_{k;n}(w_{k,j;n}, \chi_{k;n}) F_{TV}(\chi_{k;n}), \tag{12}$$

where F_{TV} is the weighted L^2-norm TV factor, viz.

$$F_{TV}(\chi_{k;n}) = \frac{1}{V} \int_D \frac{|\nabla \chi_{k;n}(\mathbf{p})|^2 + \delta^2_n}{|\nabla \chi_{k;n-1}(\mathbf{p})|^2 + \delta^2_n} \mathrm{d}v(\mathbf{p}), \tag{13}$$

where V is the area of the investigation domain D and where δ_n is an appropriately chosen positive parameter (see [11]). As the initial estimates, the contrast source $w^{inv,I}_{k,j}$ obtained from the first step are used. In each iteration, the contrast sources and the contrast are updated

alternatingly. Results show that, minimizing such a cost functional, higher order scattering effects are taken into consideration while the computational cost is only double the cost of DCSI-I. Since, in the single-frequency case, the results are superior to DCSI-I, in the following sections we will only discuss the multi-frequency case for the DCSI method II.

3. MULTI-FREQUENCY DCSI METHOD

So far, the problem has been treated considering each frequency k as a separate reconstruction process. In the following, the DCSI method II extension to the multi-frequency case will be described. From the Maxwell model of the contrast function, see Eq. (4), it follows that one unknown is dealt with (say χ_1) and the contrast at another frequency can be easily computed from χ_1 using the following operator relation relation

$$\chi_k = \mathcal{M}_{k,1}\chi_1 = \mathrm{Re}[\chi_1] + i\frac{\omega_1}{\omega_k}\mathrm{Im}[\chi_1]. \qquad (14)$$

In the multi-frequency inverse DCSI method II, we then invert all the available data simultaneously. To accommodate this, the DCSI method I is first used for all the different frequencies, separately. For every value of the contrast source, the correspondent total internal field is computed using Eq. (9). Subsequently, the following multi-frequency cost functional is defined and iteratively minimized

$$\mathcal{C}_n = F_n^{II}(w_{k,j;n}, \chi_{1;n})F_{TV}(\chi_{1;n}), \qquad (15)$$

where

$$F_n^{II} = \frac{\sum_{k,j}\|f_{k,j} - G_k^S w_{k,j;n}\|_S^2}{\sum_{k,j}\|f_{k,j}\|_S^2} + \frac{\sum_{k,j}\|\mathcal{M}_{k,1}\chi_{1;n}u_{k,j}^{inv,I} - w_{k,j;n}\|_D^2}{\sum_{k,j}\|\mathcal{M}_{k,1}\chi_{1;n-1}u_{k,j}^{inv,I}\|_D^2} \qquad (16)$$

and F_{TV} is defined by Eq. (13). Details of the actual minimization procedure of this multi-frequency cost functional are given in [5].

4. NUMERICAL RESULTS

In this section the multi-frequency extension of the DCSI method II will be validated by presenting a selection of the results of several numerical simulations.

The first geometry considered is the same as in [3] and consists of two rhomboidal-cross-section cylinders of contrast functions $\chi' = 1.0$ and $\chi'' = i1.0$ (see Figure 1). The investigation domain D of size $d = 3\lambda = 3$m has been discretized using 29×29 sub-cells. The measurement domain S is composed of 22 points equally spaced around the investigation domain on a circle of radius $d = 3\lambda$. The generated data are randomly corrupted

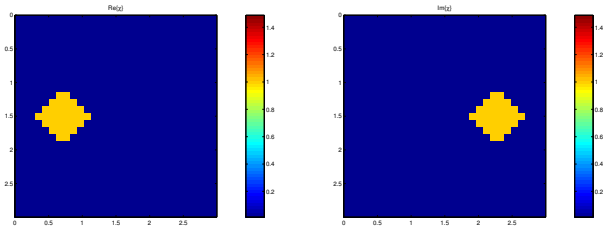

Figure 1. Actual profile of the two rhomboidal cylinders configuration plotted at 300 MHz. Real (left) and imaginary (right) part of the contrast function.

by a noise whose maximum value is given as percentage of the maximum value of the amplitude of all scattered fields recorded. For all the reported configurations the noise level is equal to 10%. The positivity constraints on the contrast functions have been applied during the minimization.

For the sake of comparison, we showed in Figure 2, the reconstruction results obtained using the single-frequency version of the DCSI method. The results are remarkable, especially considering that the computational time required by the technique is very limited. However, some inaccuracies can be noticed in the reconstructed distribution such as the overestimation of the real part of the contrast function and also the presence of

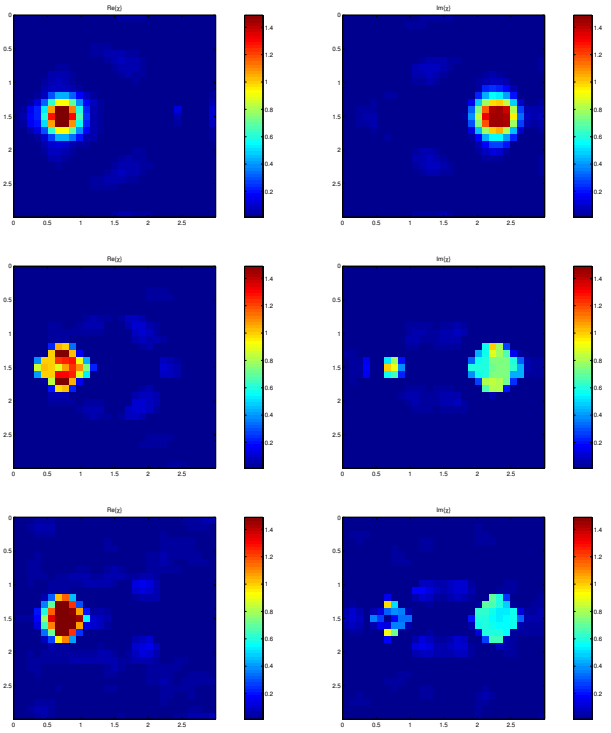

Figure 2. Single-frequency reconstruction results using data at 200MHz (top), 300MHz (middle) and 400MHz (bottom). Real (left) and imaginary (right) part of the contrast function.

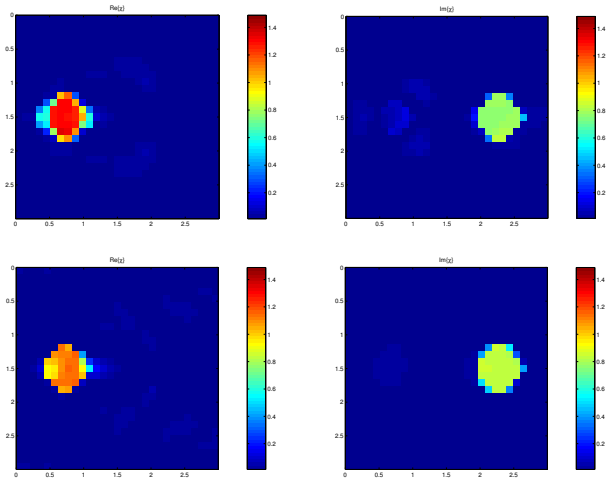

Figure 3. Simultaneous multi-frequency reconstructions of two rhomboidal cylinders after 512 iterations using 200, 300 and 400MHz data sets (top plots) and using 100, 200, 300, 400 and 500MHz data sets (bottom plots). Real (left) and imaginary (right) part of the contrast function.

small artifacts on the imaginary part of the contrast function. The reconstruction results obtained considering the different frequency data sets simultaneously are given in Figure 3. The figures show that the inversion positively benefit from the use of multiple frequency data sets. In particular, the value of the real and imaginary part of the contrast function are more accurately reconstructed and the shape of both cylinders are clearly defined. Furthermore the artifacts present on the single-frequency inversions are almost completely removed. The values and shape of the contrast can be reconstructed very faithfully using additional frequency data (see the bottom plots of Figure 3), and although the computational time depends on the number of frequencies used, the total computational burden is still less than the one needed by the single-frequency full non-linear technique. On a desktop PC, the full non-linear inversion of this configuration requires 94.23 seconds while the DCSI method only needs 12.76, 39.01 or 65.62 seconds using one, three or five frequencies. Note that, the imaginary part of the profile depends on the frequency and for the multiple-frequency reconstructions the actual value (i.e., 1.0) at the frequency of 300MHz has been used for reference.

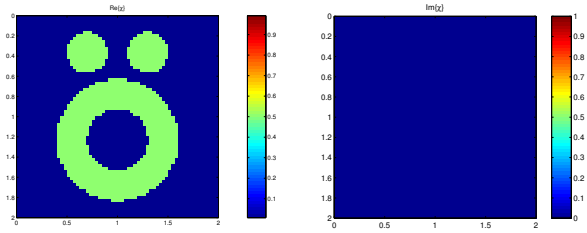

Figure 4. The actual profile of the Austria configuration. Real (left) and imaginary (right) part of the contrast function.

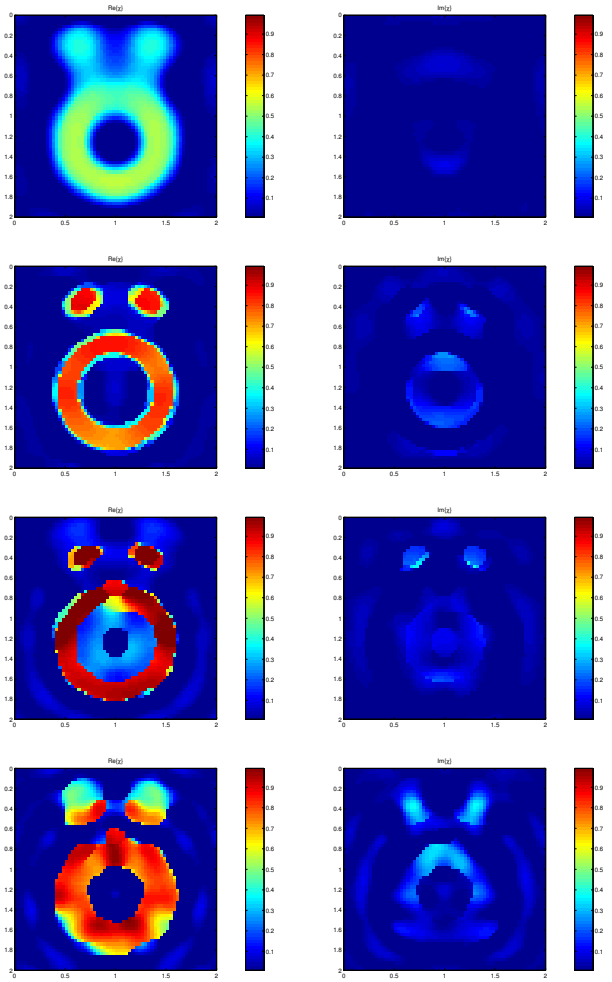

Figure 5. The single-frequency reconstruction results of the Austria configuration using data at (from the top to the bottom) 200, 300, 400 and 500MHz. Real (left) and imaginary (right) part of the contrast function.

The next numerical example reported is the so-called 'Austria' configuration. It is composed by two disks and a ring placed in a square investigation domain of side 2m, as showed in Figure 4. The two disks have radius 0.2m while the ring has an inner and outer radius of 0.3m and 0.6m, respectively. All the objects are characterized by a real contrast function $\chi = 0.5$. This time the discretization of the domain D has been performed using 63×63 square subcells while the data have been collected at 48 positions on a circular measurement domain S of radius 3m. We showed in Figure 5 the reconstruction results obtained using the single-frequency DCSI method.In this case, it is evident that at the lowest frequency (when linearization might still be valid), the reconstruction estimates correctly the value of the contrast function but fails to clearly define its boundaries. On the contrary, the highest frequency reconstruction clearly distinguish the disks and ring boundaries but overestimates their contrast function values. We therefore consider the inversion of multiple-frequency data sets of the 'Austria' con-

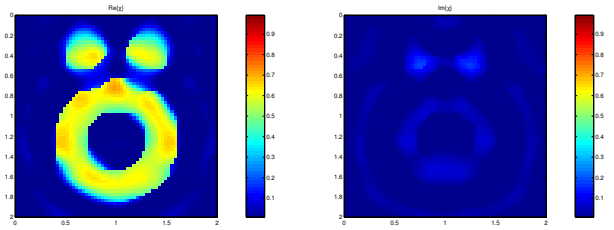

Figure 6. Simultaneous multi-frequency reconstructions of the 'Austria' configuration using 200, 300, 400 and 500MHz. Real (left) and imaginary (right) part of the contrast function.

figuration by inverting data at all four frequencies (200, 300, 400 and 500MHz) simultaneously. The reconstruction obtained is given in Figure 6. As can be seen from the figure, exploiting all the frequencies reduces the overestimation effects noticed on the single-frequency inversions. Furthermore, by combining the lower frequencies estimation of the contrast value and the higher frequencies resolution this approach allows one to effectively exploit multi-frequency data sets and obtain satisfying reconstruction for complex structure as the latter.

5. CONCLUSIONS

In this paper the multiple-frequency extension of the diagonalized contrast source inversion method has been developed in order to improve the quality of the inversion results of its single-frequency version. In particular, both hopping and multiple-frequency processing have been implemented but only the results of the latter have been reported here. The simultaneous exploitation of the multi-frequency data sets, pointed out a substantial reduction of the overestimation effects in the inversion figures noticed on the single-frequency inversion.

ACKNOWLEDGMENTS

This research was carried out by A. Casagranda at the Delft University of Technology, The Netherlands, as a part of his M.Sc.'s final project under the realm of the Socrates-Erasmus Programme.

REFERENCES

[1] M. Born and E. Wolf. *Principles of optics*. Pergamon Press, Oxford, 1980.

[2] P. M. van den Berg and R. E. Kleinman. A contrast source inversion method. *Inverse Problems*, 13:1607–1620, December 1997.

[3] A. Abubakar, T. M. Habashy, P. M. van den Berg, and D. Gisolf. The diagonalized contrast source approach: an inversion method beyond the Born approximation. *Inverse Problems*, 1:685–702, 2005.

[4] T. M. Habashy, M. L. Oristaglio, and A. T. de Hoop. Simultaneous nonlinear reconstruction of two-dimensional permittivity and conductivity. *Radio Science*, 29:1101–1118, 1994.

[5] P. M. van den Berg, A. Abubakar, and S. Semenov. A robust iterative method for Born inversion. *IEEE Transaction Geoscience Remote Sensing*, 42:342–354, 2004.

[6] T. M. Habashy, R. W. Groom, and B. Spies. Beyond the Born and Rytov approximations: A nonlinear approach to electromagnetic scattering. *Journal Geophysical Research*, 98:1759–1775, 1993.

[7] A. Abubakar and T. M. Habashy. The tensorial formulation of the diagonalized contrast source inversion method for nonlinear inversion in elastic tomography. *Proceeding of The Seventh IASTED International Conference on Signal AND Image Processing*, page 6p, 2005.

[8] W. C. Chew and J. H. Lin. A frequency-hopping approach for microwave imaging of large inhomogeneous bodies. *IEEE Microwave and Guided Wave Letters*, 5:439–441, 1995.

[9] R. F. Bloemenkamp, A. Abubakar, and P. M. van den Berg. Inversion of experimental multi-frequency data using the contrast source inversion method. *Inverse Problems*, 17:1611–1622, December 2001.

[10] D. Colton and R. Kress. *Inverse Acoustic and Electromagnetic Scattering Theory*. Springer, Berlin, 1992.

[11] P. M. van den Berg, A. Abubakar, and J. T. Fokkema. Multiplicative regularization for contrast source inversion. *Radio Science*, 38, February 2003.